Journal of Membrane Science and Research 5 (2019) 137-146

Journal of Membrane Science & Research

journal homepage: www.msrjournal.com

Research Paper

Investigation of the Improvement of Energy Generation by Pressure Retarded Osmosis

Endre Nagy *, Mónika Meiczinger, Márta Vitai

University of Pannonia, Research Institute of Biomolecular and Chemical Engineering, Lab. of Chemical and Biochemical Processes, Egyetem u. 10, H-8200, Veszprem, Hungary

Article info

Received 2018-06-28
Revised 2018-09-30
Accepted 2018-10-13
Available online 2018-10-13

Keywords

Pressure retarded osmosis
Solute transport
Water transport
Interface concentrations
Improved osmotic pressure difference

Highlights

- Overall mass transfer rate and mass transfer coefficient were defined for PRO process.
- Values of the individual interface concentrations were expressed and discussed.
- It needs strong decrease of S value to reach high maximum power density, when $B = \gamma A^3$.
- Improvement of the membrane properties can substantially increase the performance.

Graphical abstract

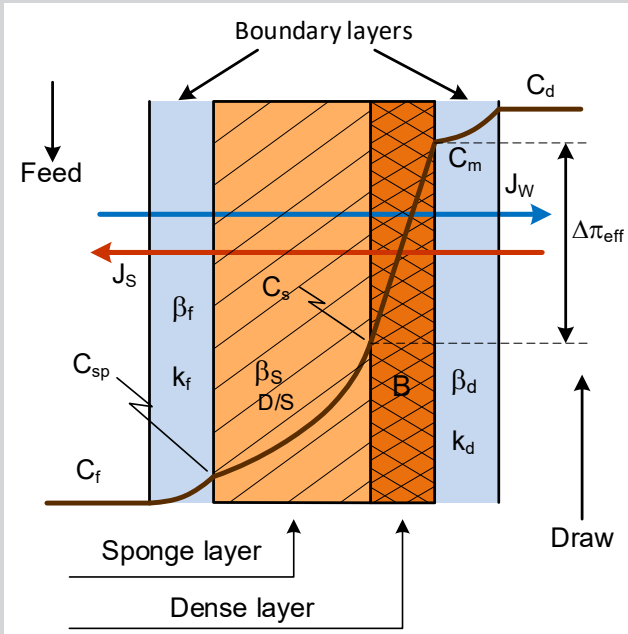

Abstract

Knowing the overall solute flux and the partial fluxes expressed by every single transport layer, the membrane internal interface concentrations can separately be expressed. Both the overall transport coefficient and the driving force strongly depend, among others, on the value of the structural parameter and the water permeability. Study of the interface concentrations as a function of the membrane characteristic properties and the operation conditions shows clearly the different, individual effects of the C_m, C_s interface membrane concentrations (and C_{sp}) on the concentration difference across the membrane active layer and thus on the process efficiency. The change of the value of C_s is much more sensitive on the membrane transport properties than that of the value of C_m. The high value of the structural parameter essentially destroys the membrane performance accordingly efforts of the manufacturers must be focused on lowering of its value for increase of the water permeability. The membrane performance can also be improved not only by its characteristic properties, but by the operating conditions as well, e.g. by applying different solute concentrations instead of seawater-river water pair. The higher draw solute or lower feed concentrations can serve then much higher power density. The knowledge of the individual interface concentration of every single transport layer enables the user to do more deep, more precise study of the mass transfer process during pressure retarded osmosis. Finally, it is shown reasonable agreement between the measured and predicted data.

1. Introduction

Osmotically driven membrane processes including forward osmosis (FO) and the pressure retarded osmosis processes (PRO) play very important roles in several industrial processes such as producing fresh water from seawater [1, 2], capturing clean energy [3, 4], water and waste water treatment [5, 6], foodstuff processing [7], etc. These promising membrane processes are intensively researched throughout the word proving by the rapidly increasing number of research papers for both the FO [8, 9] and PRO processes [10]. The PRO is a promising process for the so called blue energy generation without essential emission of CO_2. These osmotically driven processes operate on the principle of osmotic transport of water across a semi-permeable membrane from a low salinity feed solution (e.g. fresh water, river water) into a high salinity brine/draw solution (e.g. seawater, brine water) [3]. The draw solution side is pressurized to obtain power by depressurizing the portion of water permeated through the membrane from the low salinity solution in case of PRO process. The performance of these processes strongly depends on the salt- and water transport rates. The mixing of seawater (with

* Corresponding author at: Phone: 0036-20-351-8727; fax: 0036-88-624038
E-mail address: nagy@mukki.richem.hu; nagye@mik.vein.hu (E. Nagy)

DOI: 10.22079/JMSR.2018.88969.1200

about 35 g/L solute concentration) and river water (with about 3.5 g/L salt concentration) pair has theoretically 0.721 kWh/m^3 [10, 11], Most of the theoretical Gibbs free energy is lost during the present technology processes (theoretical loss of energy is 0.3 kWh/m^3, parasitic loads predicted to be 0.418 kWh/m^3) and thus, the extractable net specific energy is practically less than 0.124 kWh/m^3 [10, 11]. This about 17% of the free energy is not enough for an economic energy production by this process. That is why an essential improvement of the membrane properties and even the more accurate description and analysis of the effect on the different operating conditions should be made to find a real economic solution of this problem. Accordingly, an important step is a more accurate and extended description of the mass transport through the osmotically driven membranes, which is crucially important for correct prediction and improvement of the process performance. Straub et al. [10] recommended a RO-PRO hybrid system mixing wastewater as an alternate process. Recently Wan and Chung [12] published a techno-economic evaluation of various RO-PRO and RO-FO hybrid processes predicting the energy and cost saving by these processes with four different configurations. Other alternate methods could be the recovery of the solute enabling its repeated usage. Klaysom et al. [13] reviewed the most often used solutes (inorganic, organic, etc.) for PRO process and briefly discussed the possible methods of their recovery in order to establish a closed cycle PRO process. A cheap recovery of a solute component enables the user its repeated usage as thermolysis e.g. for degradation of ammonium carbonate compound [14]. Solidification could also be a viable separation mechanism. Precipitation can be induced through a change of pH or the addition of a flocculant, respectively [13].

Nagy et al. [15] defined the solute transfer rates for every single mass transport layer, and using them several new expressions can be obtained regarding the transport properties and also the membrane characteristics. These new expressions for the mass transport properties, showed in this paper, enable the user to develop more accurate mathematical equations, to predict e.g. more accurately the water flux, without the commonly used linear approach using van't Hoff equation and to find the most desired operating conditions.

Considering the literature data, Wang et al. [16] summarized recently the most important transport models through osmotic membranes, among them, the solution-diffusion-convection models, as well. The first paper on pressure retarded osmosis was published by Lee et al. [17] while, one of the latest one by Bui et al. [18]. Between this time periods, the mass transport models have been gradually improved taking into account the effect more and more mass transport resistances applying the solution-diffusion-convection model. Four mass transfer resistances can affect the solute and the water transport through an osmotic, asymmetric membrane, namely the selective and the support membrane layers as well as the external boundary layers on the both sides of the membrane [18, 19]. Lee's model [17] expresses the solute and water transfer rates, solute permeability coefficient, *B*, and the energy generated taking into account the effect of the two membrane layers, only. Loeb et al. [20], applying the Lee's model, have developed equation for determination of the resistance to solute diffusion in the membrane support layer, K. Later it has been proved that not only the internal (ICP) but the external concentration polarizations (ECP) can have important role in the performance of the membrane processes [21]. Accordingly, the newly developed models by McCutcheon and Elimelech [22] and by Yip et al. [23] involved already the effect of the external mass transfer resistance at the draw solution's side. This model is widely used in the literature [24, 25]. Recent investigations have shown that the concentration polarization at the low-salinity feed solution can also affect the mass transfer rate [19]. Each one of these four mass transfer resistances is taken into account in Nagy's model [15, 19] and in the recently published one by Bui et al. [18] as well as in paper of Maisonneuve [26]. Above models define the transport rates for flat-sheet membranes, only. Wan and Chung predicted the effect of the concentration change and the hydraulic pressure loss along axial direction in both the lumen and the shell side of capillary membrane in PRO process [27]. Recently, Cheng and Chung [28] investigated the effect of the cylindrical space on the transfer rates in PRO system. These models offer equations for prediction of the salt- and water transfer rates and the osmotic pressure difference. Though, they got their results in different ways, all of them give the same flux results. There is an essential difference in the mathematical methodology used by Nagy et al. [15] and Nagy [19] and the other authors. Nagy expressed the salt transfer rate for every single mass transfer layer, in his model, using the solution-diffusion-convection model, and thus, the resistance-in-series model can serve the overall salt- and water transfer rates, the concentration distribution in every layer, and the salt concentrations of the every single internal interface and the effect of the model parameters on values of them. The literature models [29, 30] do not make possible to give the individual internal interface concentrations and the concentration distributions in the different transport layers. Thus, Nagy's models can offer much more expressions to analyze the transport in every transport layer in order to get better membrane performance, and energy generation as high as possible. The knowledge of the individual interface concentration enables the reader to predict the osmotic pressure difference more precisely, namely using the C_m and C_s concentrations and from them predicting the exact values of the osmotic pressure difference by means of the e.g. OLI Stream Analyser software instead of using the van't Hoff approach.

The aim of this paper, partly, is to show the change of some new parameters and properties in the PRO process, which can be obtained by means of the solute transfer rate defined for every single mass transfer layer and by expressing the overall salt transport rate. Accordingly, this paper discusses the change of the overall mass transfer coefficient, the individual internal concentrations with their limiting cases as a function of the structural parameter and the water permeability not only for seawater and river water pair, but also higher solute concentration in the draw solution. The application of higher solute concentration in the draw solution and lower one than the river water in the feed solution the process performance can essentially be improved. This will briefly be shown in this study by means of the new model expressions. The water fluxes, obtained by means of the van't Hoff linear approach are compared to that using the individual interface concentrations of the active membrane layer and the OLI software, as a function of the water permeability coefficient, for illustration of the difference between them.

2. Theory

2.1. *Overall salt transport rate equation and interface concentration expressions*

A). Solute transfer rate.

The concentration distribution with the important nomenclature is illustrated for PRO process in Figure 1. The starting step for definition of the overall mass transfer rate is the expression of the salt fluxes given as the product of the transfer coefficient, β, and driving force for every single transport layer, namely for the selective- [Eq. (2)] and the support membrane layer [Eq. (3)] as well as for the draw [Eq.(1)] and feed side boundary layers [Eq. (4)] as they were given by Nagy [19]:

$$J_s = \beta_d\left(C_d e^{-J_w/k_d} - C_m\right) \tag{1}$$

$$J_s = -B\left(C_m - C_s\right) = -B\Delta C_m \tag{2}$$

$$J_s = \beta_{sp}\left(C_s e^{-J_w S/D} - C_{sp}\right) \tag{3}$$

$$J_s = \beta_f\left(C_{sp} e^{-J_w/k_f} - C_f\right) \tag{4}$$

where

$$\beta_d = \frac{J_w}{e^{-J_w/k_d} - 1} \tag{5}$$

$$\beta_{sp} = \frac{J_w}{e^{-J_w S/D} - 1}$$

$$\beta_f = \frac{J_w}{e^{-J_w/k_f} - 1}$$

Note that *D* denotes here the solute diffusion coefficient in the draw solution, while *S* expresses the real diffusion path in the membrane support layer, namely $S=\delta\tau/\varepsilon$, where δ means the thickness of the support layer, τ is the tortuosity factor, ε is the hold-up of the support layer. Literature often uses K parameter, which is the transfer resistance of the support layer, where: $K=S/D\equiv\delta\tau/(\varepsilon D)$.

Applying any conventional method using the above equations, the overall salt transfer rate, which involve the effect of every transport layer, can be expressed as:

$$J_s = \beta_{ov}\left(C_d - C_f e^{J_w\left(1/k_d + 1/k_f + S/D\right)}\right) \tag{6}$$

where

$$\frac{1}{\beta_{ov}}=\frac{1}{J_w}-\frac{e^{J_w/k_d}}{B}-\frac{e^{J_w\left(1/k_d+1/k_f+S/D\right)}}{J_w} \tag{7}$$

Note that the above expression is essentially differs from that given in the previous paper of Nagy et al. [15] since here the concentration of the draw solution has not the factor of $\exp(-J_w/k_d)$. That form of literature mass transfer rate equation was usually used for gas-liquid systems. It can clearly be seen how the driving force depend on the ratio of the convective and diffusive fluxes (i.e. on the Peclet number of the transverse mass transport). It is obvious that the driving force decreases with the increase of the water flux. One can easily express the overall mass transfer rate without convective velocity, k_{ov}, as *lim* β_{ov} when $J_w\to 0$:

$$\frac{1}{k_{ov}}=-\left(\frac{1}{B}+\frac{1}{k_d}+\frac{S}{D}+\frac{1}{k_f}\right) \tag{8}$$

The overall transport coefficient, β_{ov}, is always less than the overall diffusive mass transfer coefficient due to the reverse convective velocity. The solute transfer rate expressing by means of the concentration difference across the selective layer can also be expressed as it is given in the literature [11, 19]:

$$J_s=B\left(C_m-C_s\right)=\frac{B\left(C_d e^{-J_w/k_d}-C_f e^{J_w\left(1/k_f+S/D\right)}\right)}{1+\frac{B}{J_w}\left(e^{J_w\left(1/k_f+S/D\right)}-e^{-J_w/k_d}\right)} \tag{9}$$

Multiplying both the nominator and the denominator of Eq. (9) by $\exp(J_w/k_d)$ expression, one can get the value of β_{ov} expressed by Eq. (7).

B) The internal interface concentrations.

Determination of the interface concentrations, namely values of C_m and C_s enables the user to study their individual dependence on the water and solute fluxes. After simple manipulations of the partial and overall salt transfer rates these concentrations can easily be obtained. Applying the equality of the solute transfer rates, expressed by Eq. (1) and Eq. (6), the expression of C_m can easily be obtained as:

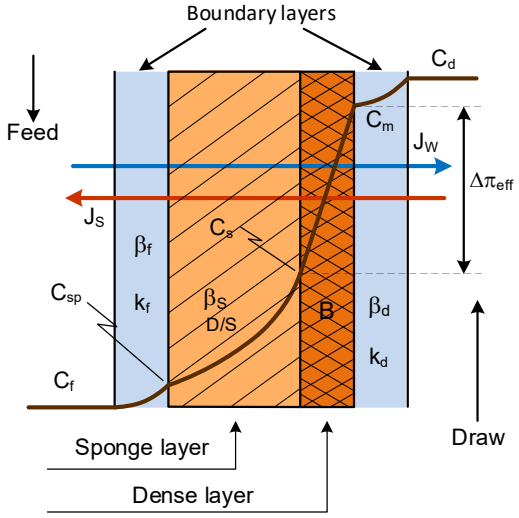

Fig. 1. Illustration of salt concentration profiles and giving the denotes and mass transfer coefficients in case of asymmetric membrane for pressure retarded osmosis taking into account both the external and internal polarization layers. $\Delta\pi_{eff}$ means the effective osmotic pressure. Its value can be determined by difference of the interfacial membrane concentration. The β mass transfer coefficients (β_d, β_{sp}, β_f are mass transfer coefficients in presence of convective water flux while k_i (i=d, f, sp) is the diffusive mass transfer coefficient).

$$C_m=\frac{C_d\left\{1+\frac{B}{J_w}\left(e^{J_w\left(S/D+1/k_f\right)}-1\right)\right\}e^{-J_w/k_d}+C_f\frac{B}{J_w}\left(1-e^{-J_w/k_d}\right)e^{J_w\left(S/D+1/k_f\right)}}{1+\frac{B}{J_w}\left(e^{J_w\left(S/D+1/k_f\right)}-e^{-J_w/k_d}\right)} \tag{10}$$

The limiting value of the C_m namely when $B\to 0$ tends to expression of $C_{m,J_s=0}=C_d\exp\left(-J_w/k_d\right)$

Determination of the value of C_s e.g. the following salt flux can be used obtaining from expressions of Eqs. (1) and (2), namely:

$$J_s=\beta^*\left(C_d-C_{sk}e^{J_w/k_d}\right)\ \text{with}\ \frac{1}{\beta^*}=\frac{1}{\beta_d}-\frac{e^{J_w/k_d}}{B} \tag{11}$$

Then the value of C_s can then be defined by means of Eqs. (6) and (11), as:

$$C_s=\frac{C_d\left\{\frac{B}{J_w}\left(e^{J_w\left(S/D+1/k_f\right)}-1\right)\right\}e^{-J_w/k_d}+C_f\left\{1+\frac{B}{J_w}\left(1-e^{-J_w/k_d}\right)\right\}e^{J_w\left(S/D+1/k_f\right)}}{1+\frac{B}{J_w}\left(e^{J_w\left(S/D+1/k_f\right)}-e^{-J_w/k_d}\right)} \tag{12}$$

It is easy to get the limiting values of the C_s from Eq. (12), when B→0 [Eq. (13) when C_f >0] or C_f=0 [Eq. (14) when B > 0] or both the values of B and C_f are equal to zero, i.e. when B=0 and C_f=0 then C_s=0. In this latter case there is no ICP and ECP on the feed side. Obviously this ideal case could serve the maximum value of energy. Eq. (14) clearly shows that ICP and ECP can form on the feed side even then when C_f=0, but B>0, due to the solute transport through the selective membrane layer.

$$C_s = C_f e^{J_w(1/k_f+K)} \tag{13}$$

$$C_s = \frac{C_d\left\{\frac{B}{J_w}\left(e^{J_w(S/D+1/k_f)}-1\right)e^{-J_w/k_d}\right\}}{1+\frac{B}{J_w}\left(e^{J_w(S/D+1/k_f)}-e^{-J_w/k_d}\right)} \tag{14}$$

The widely used salt transfer rate given for the selective layer without (see Ref. [22]) and with external transfer resistance(s) (see Ref. [11, 19]), namely J_s=-B(C_m-C_s), can easily be obtained by Eqs. (10) and (12), as it is expressed by Eq. (9). Similarly, the solute transfer rate for limiting case, namely when B=0, can easily be obtained from Eqs. (10) and (12) or by means of Eq. (16) with B→0.

The water flux can then be expressed by the commonly used linear approach as (the osmotic pressure, π=iMCR$_g$T where *i* is van't Hoff dissociation factor (it is 2 for NaCl), C salt concentration, M molecular weight, R_g gas constant, T temperature) [9, 30]:

$$J_w = A\left(\Delta\pi_m - \Delta P\right) \tag{15}$$

where ($\Delta\pi_m$ is the effective osmotic pressure difference across the selective layer, $\Delta\pi_m$; see value of $\Delta\pi_{eff}$ in Figure 1)

$$\Delta\pi_m = \frac{\left(\pi_d e^{-J_w/k_d} - \pi_f e^{J_w(1/k_f+S/D)}\right)}{1+\frac{B}{J_w}\left(e^{J_w(1/k_f+S/D)}-e^{-J_w/k_d}\right)} \tag{16}$$

The osmotic pressure difference can also be expressed by more accurate method, obtaining the osmotic pressure difference using the individual interface concentrations as well as:

$$\Delta\pi_m = \pi_m\left(C_m\right) - \pi_s\left(C_s\right) \tag{17}$$

The single values of $\Delta\pi_m$ and $\Delta\pi_s$ were predicted by means of the OLI Stream Analyiser software [31]. Both model results are compared in separate figures. Concentration of interface between the support and the feed boundary layer,

C_{sp} can then be defined similarly to the method used for determination of the other interface concentrations, as

$$C_{sp} = \frac{C_d\left\{\frac{B}{J_w}\left(e^{J_w/k_f}-1\right)e^{-J_w/k_d}\right\}+C_f\left\{1+\frac{B}{J_w}\left(e^{J_w S/D}-e^{J_w/k_d}\right)\right\}e^{J_w/k_f}}{1+\frac{B}{J_w}\left(e^{J_w(S/D+1/k_f)}-e^{-J_w/k_d}\right)} \tag{18}$$

Eq. (18) gives direct answer to the reader how the resistance of the support layer affects the process performance. Concentration fall across the different transport layers, namely the external polarization layer (ECP) on the draw side, selective layer, the support layer and the ECP on the feed phase [20] can then easily be given by means of Eqs. (10), (12) and.(18)

Question can arise why the individual, relative complicated concentration expressions can be important. That is why, to our opinion, these expressions enable the user to investigate the change of the interface concentrations separately, thus more deeper and more accurate information can be obtained on the effect on the membrane properties and operation conditions in PRO process considering its performance under different conditions.

3. Evaluation method

The mathematical model presented defines some new variables, namely the transport coefficient of the single transport layers, β_L (*i*=s, f, sp), the overall transport coefficients, β_{ov} and the interface solute concentrations of the solute. The resistance-in-series model [19] enables the user to do much deeper study of the mass transport properties of the PRO (and FO systems; not discussed here) than that of the conventional literature models, which apply the equality of the inlet and the outlet solute fluxes at a given transport boundary, for determination of the mass transfer expressions, but this methodology cannot define the individual solute fluxes. Knowing the concentration of every single internal interface, the concentration distribution in every layer, the overall mass transfer rate and even the transport coefficient using the solution-diffusion-convection and every mass transfer resistance can be defined and studied. These can help the user to predict exactly the effect of all transport layers thus, one can easier find harmony between the membrane properties and operating conditions in order to get as high as possible value of the water flux and thus, value of the harvestable energy. Knowledge of the new variables defined, especially the C_m C_s C_{sp} interface membrane concentrations, enables the user the deeper analysis of the process performance. On the other hand, the knowledge of these interface concentrations is necessary for more exact prediction of the osmotic pressure difference on the selective layer due to the osmotic pressure's nonlinear property as a function of the solute concentration as it is the case in NaCl solution. This is especially important at high concentration of draw solution facing the active membrane layer. Illustration of the difference between the linear approach and our model is illustrated first then the changes of the interface concentrations and the transport coefficient are shown in the first part of this study. Then the effect of extreme values of the solute permeability (B → 0) and the feed solute concentration (C_f→0) will be shown as well as the effect of the external mass transfer coefficients and the concentration of the draw solution are briefly discussed.

The starting expressions used give the same transport flux as the literature ones. The osmotic pressure difference can be predicted more accurately, applying the individual interface concentrations according to Eq..(17) The difference between the linear approximation (van't Hoff equation) and the presented expression can even reach 25%. The predicted results are compared to the measured ones at the end of this paper and also in previous ones of authors [15, 19]. Results discussed in this paper are focusing on how the concentration conditions, the membrane performance can be affected by the membrane properties and the solute concentrations.

4. Results and discussion

In this section the change of some newly defined parameter as overall transport coefficient, interface concentrations and water flux, under even extreme conditions, will be shown. The main aim of this study is to show that the extreme solute concentrations of both the draw and feed solutions can be a real alternative method to seawater-river water pair, for economic energy production by PRO systems.

4.1. Illustration of the deviation between the linear approach and the correct prediction of the osmotic pressure difference

We think that it is important firstly to show why our new expressions regarding the single interface concentrations might be considered to be essential. Figure 2 illustrates the change of the water flux, as a function of the water permeability as characteristic intrinsic membrane parameter, obtained by the two different methods. Applying the van't Hoff expression (π=2R_gTC), the water flux obtained is remarkable higher than that obtained by the Eq. (17) with the OLI software [31] (it is called here as correct results) applying the seawater-river water pair of the draw and the feed solutions, respectively. In this low concentration range the linear approach gives higher osmotic pressures than the OLI software. Depending on the water permeability the deviation can reach even the 25%. It increases with the increase of the water flux. Knowing the value of the hydraulic pressure difference (*ΔP*=10 bar in

our case), the power density can easily be predicted in the both cases. This is evidently shows that disregarding this can cause essential error in the prediction of a membrane performance. The detailed discussion of this effect is not an aim of this paper, only task is in this paper to emphasize the importance of the model developed and analyze its effect in this paper. Additionally, the change of the interface concentration of the membrane active layer, namely C_m and C_s is shown in Figure 3, as a function of the water permeability. Interesting to note that though the C_m-C_s concentration difference is always lower in the case of the linear approach, against that the water flux is higher in case of the van't Hoff approach. This is caused by the different osmotic pressure difference at a given concentration value. On the other hand, this figure also shows that the role of the support layer increases due to the increase of the water flux. The concentration difference at the two sides of the support layer changes between about 0.035 and the value of C_s as it can be seen in this figure. The raising water flux decreases the solute flux, which increases the resistances of the external boundary layers. This can then cause decrease of the C_m value with increasing A value.

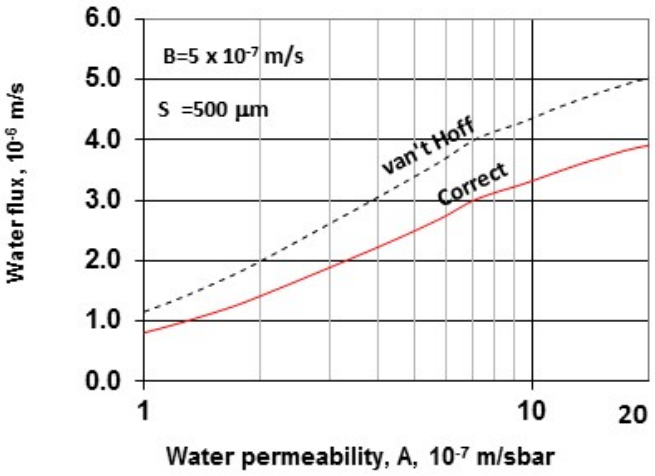

Fig. 2. Water flux as a function of the water permeability obtained by the linear approach (with van't Hoff expression) and by means of Eq. (17) using the OLI Stream Analyzer software for predicting the single π_m and π_s interface osmotic pressures (β_d=β_f= 3.85 x 10^{-5} m/s; A=1.9 x 10^{-7} m/sbar; B=5 x 10^{-7} m/s; S=500 µm; ΔP=10 bar; C_d= 0.6 kmol/m^3; C_f=0.015 kmol/m^3; [seawater/river water pair]).

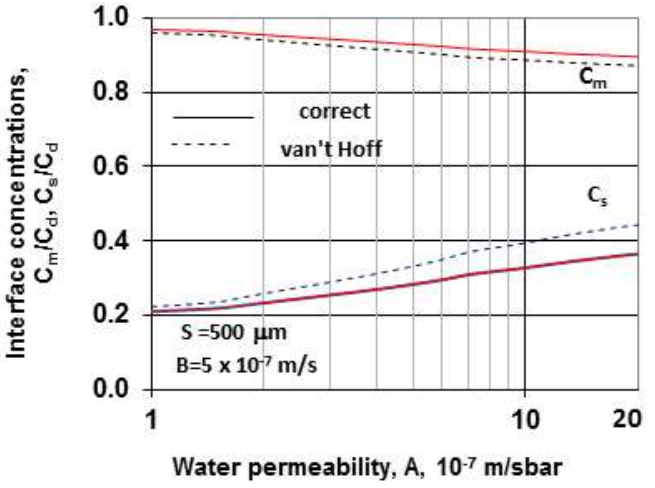

Fig. 3. The variation of the interface concentration of the active layer as a function of the water permeability. (Parameter values are given in caption of Figure 2).

4.2. Effect of the structural parameter

In this section the change some important new variables as a function of the structural parameter will be discussed. As it is known, the intrinsic properties of a membrane layer, namely membrane structural parameter, water- and solute permeability's, should essentially be improved for economic energy production. Unfortunately the recently available polymeric membranes have not possessed the desired properties yet. It is crucially important to decrease of the value of the structural parameter. Values of A and B pair were chosen according to Eq. (19) for our prediction, while the value of ΔP was selected to provide the maximum power density to the given A and B parameter-pairs. Hereinafter all predicted data are obtained using the empirically related expression between the water permeability coefficient, A, and salt permeability coefficient, B, which was developed for polymeric membranes [33], namely:

$$B = \gamma A^3 \tag{19}$$

where γ is a fitting parameter. Experimental data using polyamide membranes have been fitted to this relationship and found γ=0.1724 x 10^{-6} s^{2}bar^3/m^2 (= 0.0133 m^4 h^{2}bar^3/L^2). The cubic dependence of salt permeability on the water permeability indicates that the increase of the water permeability coefficient will rapidly decrease the selectivity of the membrane [34]. Thus, accepting this A versus B function, an important task of the producers should be to lower significantly the value of the γ preparing new industrial membrane [15].

4.2.1. Overall transport coefficient, β_{ov}

The role of the solute transfer rate is crucially important for determination of the process efficiency of a PRO system. Its definition by Eq. (6) exactly shows the effect of both the overall transport coefficient and the driving force, in presence of both the diffusive and the convective flows. It is obvious, that these overall transport coefficients, in presence of diffusive plus convective fluxes should be less than that without convective velocity, k_{ov} due to the reverse direction of the two flows. The change of the ratio of the overall transport and the overall diffusive mass transfer coefficients, β_{ov}/k_{ov} (*lim* β_{ov}=k_{ov} when $J_w \to 0$) as well as the relative value of the driving force, $\Delta C^*/C_d$, $\left\{\Delta C^* = C_d - C_f\left(J_w\left[1/k_f + 1/k_d + S/D\right]\right)\right\}$ according to Eq. (6)], are illustrated in Figure 4 in the case of different values of solute and water permeability, their function was calculated according to Eq. (19), as a function of the membrane structural parameter, S. As can be seen in Figure 4, the values of β_{ov}/k_{ov} significantly decreases, especially at higher solute permeability, while the driving force, ΔC^*, significantly increases, with the increase of the solute permeability depending on the structural parameter. The value of β_{ov}/k_{ov} (note *lim* β_{ov} = k_{ov} when $J_w \to 0$) strongly decreases as function of S and also with the increase of the value of B, though the absolute value of β_{ov} increases with the value of B .Note that the solute permeability is part of the overall transport coefficient or its reciprocal value is portion of the overall transport resistance. Normally, the value of B can be considered as the solute mass transfer coefficient of the selective layer (however it involves the solute solubility as well [16]).Value of B can generally vary between (0.03-3) x 10^{-6} m/s, as a function of A in our case, depending on the membrane characteristics. This value is at least one order of magnitude lower than e.g. that of the external boundary layers. The decrease of the value of β_{ov}/k_{ov} indicates the increasing effect of the water flux, thus its rising affects strongly the value the transport coefficient. The driving force changes mostly in the higher structural parameter range, namely between *S*=100-1000 µm. Depending on the B values it can decrease or increase as well. What is worthy to mention, the effect of the driving force on the solute transfer rate is generally significant, though it depends on the membrane properties. The J_s value lowers from 3.6×10^{-6} kg/m^{2}s down to 1.19×10^{-6} kg/m^{2}s in the structural parameter regime investigated.

The water permeability is the other crucially important intrinsic membrane parameter, which can decisively determine the efficiency of a PRO process. Its effect is illustrated in the next figure (see Figure 5). As it follows from Eq. (19), the solute permeability and accordingly the solute flux essentially increase as a function of the water permeability, accordingly of the water flux. Due to it, both the overall transport-, the diffusive mass transfer coefficients as well as the solute flux significantly increases as a function of value of A. As a result, the water flux has maximum value as a function of the water permeability, i.e. the value of J_w starts to decrease after a certain value of A due to the high solute flux. This fact clearly shows that the value of B should be limited with the increasing value of A in order to get higher water flux. The correct mass transfer expressions enable the user to predict correctly the membrane performance. The effect of the structural parameter and the

water permeability (and accordingly the solute permeability) clearly shows that the improvement of the membrane characteristics, namely the decrease of the value of S and B as well as the increase of value of A are important future task of the membrane producers.

4.2.2. Change of the interface concentrations of the active membrane layer

Values of C_m and C_s are crucially important in the efficiency of the pressure retarded osmosis. Their difference determines the osmotic pressure difference and thus, water flux and accordingly, the power density, which can be generated during this process. Knowledge of their individual values can significantly help the reader to choose the so called optimal operating conditions in order to get the desired value of energy. Change of values of C_m/C_d and C_s/C_d, at the maximum energy production, using again the A and B value pair obtaining by Eq. (19), are plotted in a three dimensional (3D) diagram to illustrate the joint effect of the values of A (and B parameter pair) as well as S (see Figure 6). Dependency of the relative values of C_m and C_s on these parameters is significantly different. Value of C_m/C_d remains above 0.8 in the whole range investigated (see Figure 4-A), while value of C_s/C_d gradually varies practically between zero and about 0.9 (see Figure 6-B). Value of C_m/C_d slightly decreases with decreasing value of S and at lower values of A. This change is somewhat stronger with decreasing value of S, and at high values of A. It has minimum value at about $S=200\times100^{-6}$ m. Change of value of C_s/C_d shows a convex surface in 3D diagram with increasing slope as a function of increasing A and also S values. It is obvious from these figures (see Figures 6-A and 6-B) that the most important task of the producers/users may be the careful choice of the value of the structural parameter at a given value of A, for getting desired osmotic pressure difference because the ICP (together with the feed side ECP) can affect the membrane performance several times stronger than that of the ECP on the draw side.

4.2.3. Water *flux under extreme conditions, namely at* $B=0$ *and* $C_f=0$

As it was already mentioned, the solute permeability and even the feed's solute concentration can have essential influence on the process performance. The solute permeability is an intrinsic property of the membrane, its value depends basically on the producers. As it is shown by Eq. (19), the solute permeability is proportional with the water permeability using polyamide/polymeric membrane.

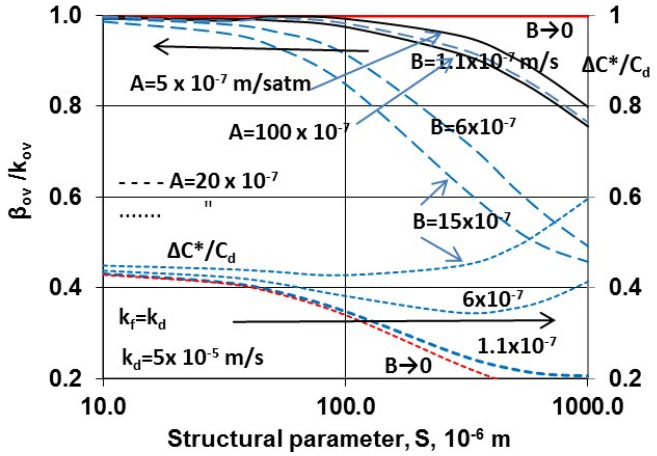

Fig. 4. The relative values of the overall mass transfer coefficient, β_{ov}/k_{ov} and driving force $\Delta C^*/C_d$ as a function of the structural parameter at different values of solute and water permeability. (C_d=58.5 g/L; C_f=2.35 g/L, ΔP=5 bar; D=1.5 x 10^{-9} m^2/s;. $\left\{\Delta C^* = C_d - C_f\left(J_w\left[1/k_f + 1/k_d + S/D\right]\right)\right\}$

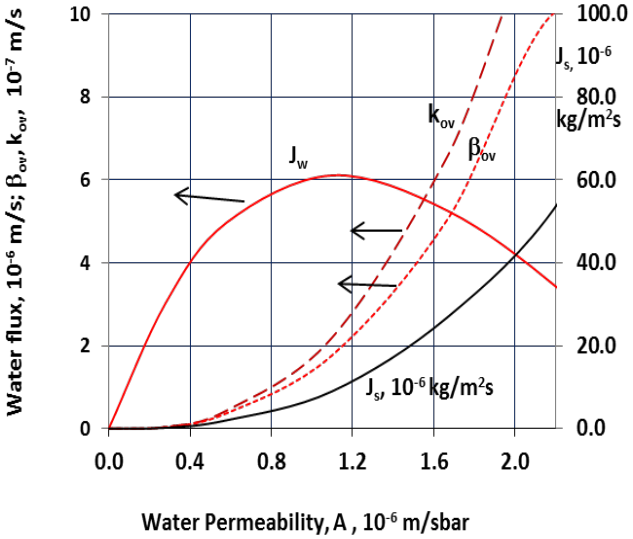

Fig. 5. The effect of the water permeability on values of the important mass transport parameters. (S=300 x 10^{-6} m; $B=\gamma A^3$; other parameters are listed in Table 1).

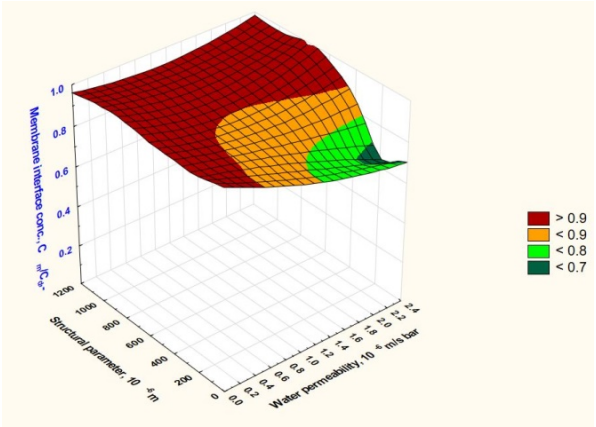

A

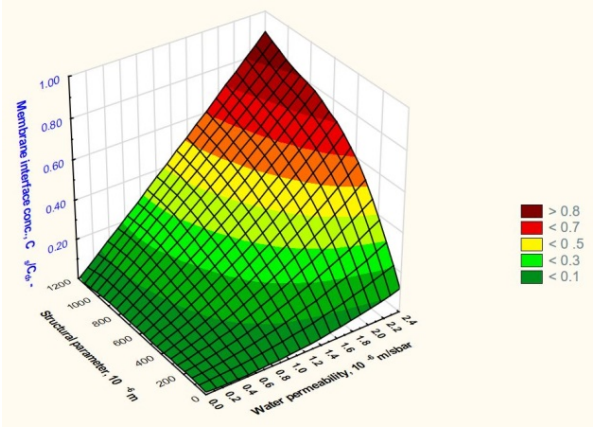

B

Fig. 6. Values of interface concentration of the active layer, C_m and C_s as a function of water permeability and structural parameter. Values of A and B pairs was calculated according to Eq. (19). Value of ΔP used for calculation of the maximum energy density belongs to the $dW/d\Delta P=0$ as a function of ΔP (W means the generated energy; for other parameters, see Table 1).

Figure 7 illustrates its significant effect on the water flux at different feed concentrations, namely C_f/C_d is varied between 0 and 0.1, and at B=0. Values of parameters are listed in Table 1. This figure clearly shows the enormous effect of the feed concentration on the membrane performance. As it perhaps obvious, without solute transport, the water flux hardly changes as a function of the structural parameter (curves with C_f/C_d=0). But a very little change of its value induces very big decrease in the water flux depending on the S value. These results clearly show the importance of the feed concentration. Its value should be chosen as low as possible. Accordingly the application of rainy water could be recommended in a PRO technology instead of river water. The feed side concentration of the membrane active layer, C_s, is also plotted (broken lines) in Figure 7. Its value remains practically zero at C_f=0 (red broken line) (the value of C_m/C_d remains about 0.48 in the whole range of the S value, at C_f=0; not shown here), but its value quickly rises with increasing feed solute concentration decreasing the osmotic pressure difference with it. Though the value of C_m also increases with increasing S, the concentration difference on the selective layer, C_m-C_s, decreases with the increase of S when B > 0.

How the B value affects the water flux at C_f=0 is plotted in Figure 8. The effect on water flux is similar to that of the feed concentration. Large B value can strongly lower the membrane performance. This effect is particularly big at higher values of S. The relatively high value of B of the currently available commercial membranes can only be balanced by higher (much higher than that of seawater) solute concentration of the draw solution. This can be realized only then e.g. when the draw solution can repeatedly applied after its regeneration.

4.2.4. Effect of the external mass transfer coefficients on the interface concentrations of the active layer

The resistance of the external mass transfer coefficients can strongly affect the osmotic pressure difference and thus the membrane performance. Especially, the draw side mass transfer coefficient has remarkable effect on the solute concentration distribution. In the interest of a more simple application, their values are often neglected as it is done e.g. in Ref. [27]. The effect of the external mass transfer coefficient pairs (β_d=β_f) is illustrated in Figure 9, at three different mass transfer coefficient pairs, namely β_i=10 x 10^{-5} m/s; 3.85 x 10^{-5} m/s and 1×10^{-5} m/s (*i*= d and f). The effect of the β is significant on both sides of the active layer. Gradual decrease of the difference between the two concentrations lowers the osmotic pressure difference. But the increase in the value of A overbalances this effect, and value of J_w is increasing at a given value pair of β. Water flux varies between 0.6×10^{-6} m/s and 2.25×10^{-6} m/s as well as between 0.861×10^{-6} m/s and 4.49×10^{-6} m/s in the A range investigated, at β_d=β_f= 1×10^{-5} m/s and β_d=β_f= 10×10^{-5} m/s, respectively. With increasing value of the water permeability, the deviation in the water fluxes can reach 100%, in the transfer rate's range investigated.

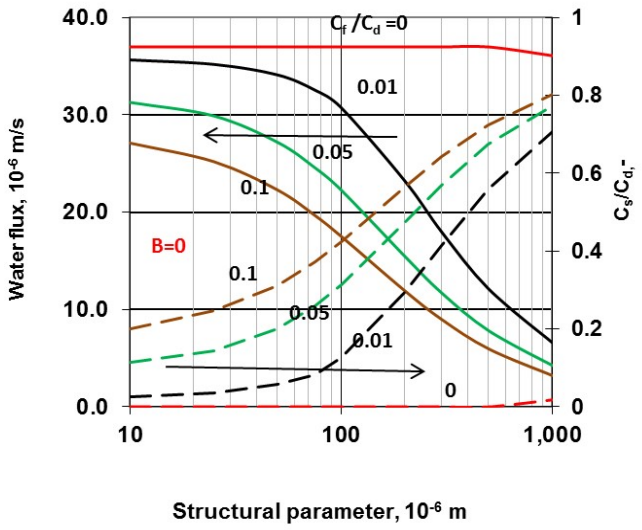

Fig. 7. Water flux as a function of the structural parameter, at extreme B value, namely B=0 (A=20 x 10-7 m/s bar; other parameters are listed in Table 1.

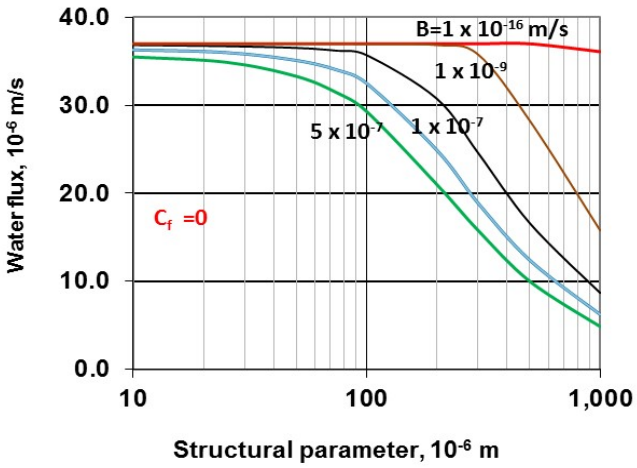

Fig. 8. Water flux as a function of the structural parameter applying solute free feed solution, C_f=0 (A=20 x 10^{-7} m/s bar; other parameters are listed in Table 1).

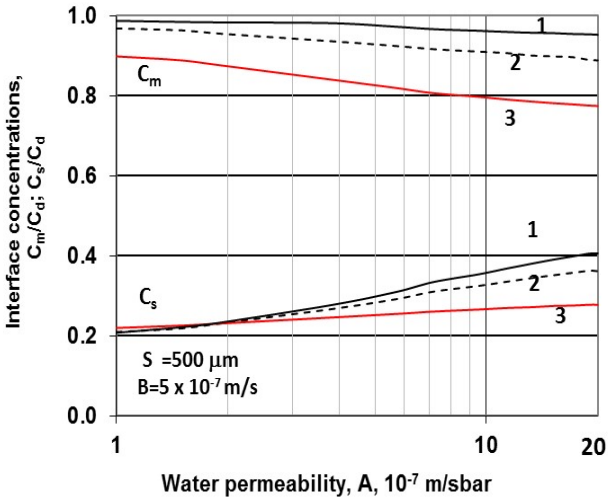

Fig. 9. The effect of the external mass transfer coefficients on the water flux as a function of the water permeability (β_i=1 x 10^{-4} m/s [curves 1]; 3.85 x 10^{-5} m/s [curves 2] and 1 x 10^{-5} m/s [curves 3];i= d, f; other parameters ar given in caption of Figure 2).

4.2.5. The effect of the inlet draw concentration on the water flux

The expression given in this paper are defined for constant draw and feed concentrations. In the reality these concentrations varies in axial direction of the capillary module. Accordingly, the effect of the concentration's change can be important in pilot-scale industrial equipment. This study does not investigate the process in industrial scale. It will be the task of a separate paper. E.g. Wan and Chung [27] discussed this effect neglecting the external mass transfer resistances. For illustration of the effect of the draw solution concentration on the water flux is illustrated in Figure 10. It is clearly seen that the concentration change has strong influence on the membrane performance. 5% concentration change induces 210% of change, in the water flux, at the beginning of the investigated concentration regime, and 52% change in the water flux, at the end of this concentration range. Accordingly, the concentration change can be recommended to be taken into account, in industrial application of the PRO process.

4.2.6 Maximum power density

The power density, W, as it is known, has maximum value as a function of the hydraulic pressure difference under given operating condition. Theoretically to reach it, a hydraulic pressure, which is approximately half of the osmotic pressure difference across the membrane [i.e. $\Delta P \cong (\pi_d - \pi_s)/2$],

should be applied [17]. The value of ΔP to which the maximum power density belongs, however, can strongly depends on the mass transfer resistance of the polarization layers. Yip and Elimelech [34] showed the value of the maximum energy as a function of the membrane properties, namely A A, B, and S, in Descartes coordinate system, determined by solving numerically $dW/d\Delta P=0$ and applying $W=J_w\Delta P$ for the determination of the maximum value of the specific energy [33]. The hydraulic pressure difference, which can provide maximum power density was varied between 5 and 13.5 bar with decreasing value of A or decreasing value of S, in the whole parameter ranges investigated, for seawater/river water pair (see Figure 11). In this work, the maximum power density was calculated in presence of feed side ECP and results are plotted in Figure 11 in a three dimensional diagram, which might be much more informative than a 2D one. Let us look at one typical point of this figure: A=1.8 x 10^{-6} m/s bar (=6.6 $Lm^{-2}h^{-1}bar^{-1}$), S=300 x 10^{-6} m then maximum power density=7.5 W/m^2 as it is presented in Figure 11. Figure 11 shows very clearly how the maximum energy density changes as a function of the S and A (as well as B according to Eq. (19)). Given values of power density ranges are clearly seen in this figure, as a functions of A (and B) as well as S, due to their different colors. As can be seen, the power density surface has a strong convex form and its maximum is shifted in direction of increasing value of A when the value of the structural parameter decreases. Accordingly, this figure can help to choose the desired value of A, depending on the value of the structural parameter, in the case when A vs. B functions corresponds to Eq. (19).

4.3. Comparison of the experimental and simulated data

Simulation data should be compared to experimental ones to be proved the correctness of the calculated data. The experimental data were taken from published data of Li et al. [35]. They prepared thin film composite polyetherimide (PEI) membranes, which were synthesized by interfacial polymerization preparing flat sheet PRO membranes. Characteristic parameters of the prepared membrane (water permeability, salt permeability, membrane structural parameter) were predicted by commonly used literature expressions, which neglect the effect of the external mass transfer resistances in paper cited. As it is illustrated in Figure 9, the effect of the external mass transfer coefficients on the membrane performance can be neglected at extremely high values of the mass transfer coefficients, only, as the C_m value shows it by curve 1. The measured data of water flux obtained by membrane PEI-2# (they are plotted in Figure 4-A, and the characteristic data are given in Table 2 in their paper [35]) are used for the calculation (see Table 2 for these data). The three measured water fluxes and the predicted ones are listed in Table 2. The measured and the calculated data show reasonable agreement proving that the calculated data shown in the previous figures can be considered as real ones.

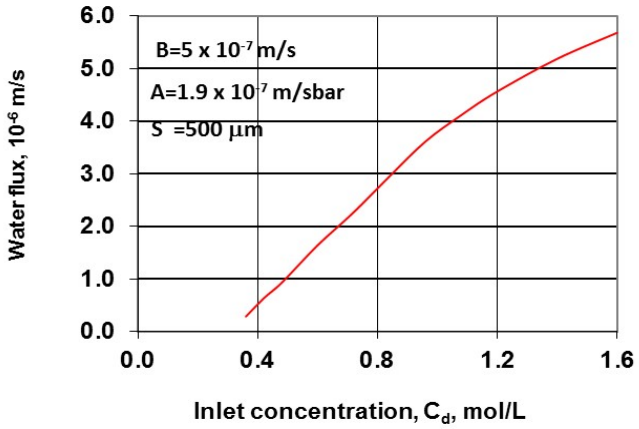

Fig. 10. Effect of the inlet draw concentration on the water flux (B=5 x 10^{-7} m/s; A=1.9 x 10^{-7} m/sbar; S=500µm; other parameters are given in caption of Fig. 2).

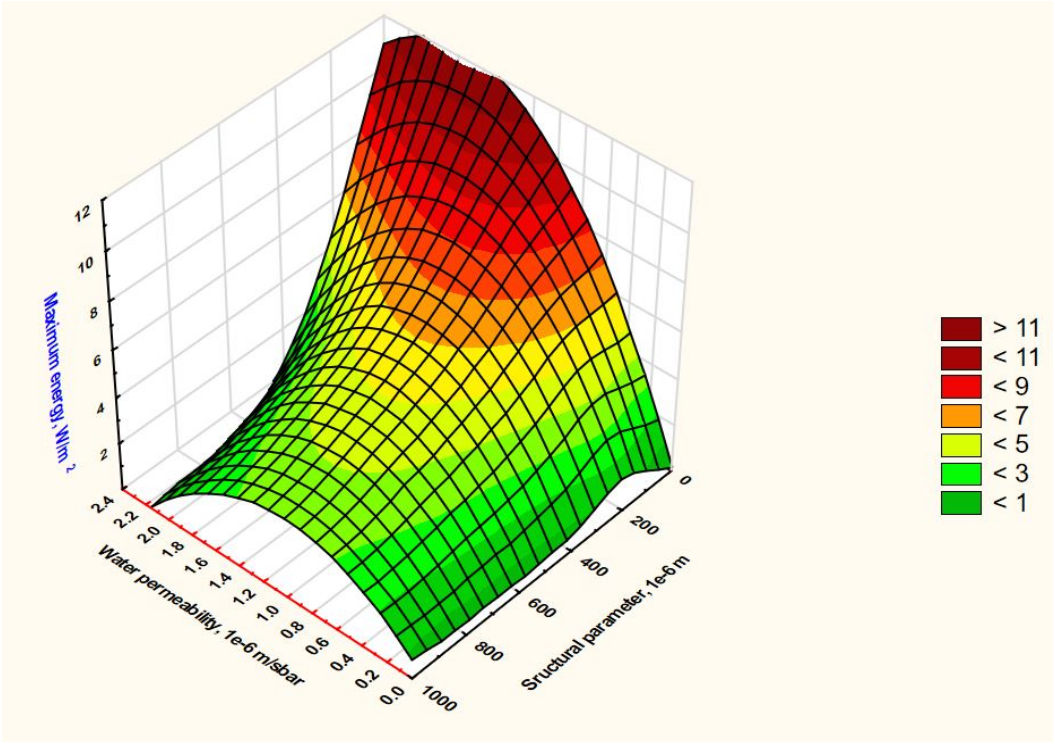

Fig. 11. Maximum energy density as a function of water permeability and the structural parameter of the membrane support layer. Values of A and B pairs was calculated according to Eq. (19). Value of ΔP used for calculation of the maximum energy density belongs to the $dW/d\Delta P=0$ as a function of ΔP (other parameter values are listed in Table 1).

Table 1
Main values of parameters used for calculation.

Simulation data	
Figs. 4, 7, and 8	Figs. 5, 6, and 11.
k_d=5 x 10^{-5} m/s;	3.85 x 10^{-5} m/s
k_f=k_d; $k_f \rightarrow \infty$	k_f=k_d; $k_f \rightarrow \infty$
S=(10-1000) x 10^{-6} m;	350 x 10^{-6} m
A=(0.5 -10) x 10^{-7} m/(s bar)	A=1.1 x 10^{-6} m/sbar (=3.96 L/m^{2}hbar)
B=1.1 x 10^{-7} m/s;	B =γA^3
C_f=2.35 g/L ($\rightarrow \pi_f$ =2.0 bar); C_f/C_d=0.04017	$C_{f,d}$=0.73 g/L ($\rightarrow \pi_f$ =0.564 bar);
C_d=58.5 g/L ($\rightarrow \pi_b$=49.2 atm)	$C_{d,b}$=35.1 g/L ($\rightarrow \pi_b$=26.14 bar)
ΔP=5 bar	ΔP=12 bar

Table 2
Comparison the experimental ([35] obtained by PEI-2# membrane) and simulated water flux.

Hydraulic pressure difference, ΔP (bar)	Water flux, 10^{-6} m/s (=3.6 L/m^{2}h)	
	Measured data	Predicted data
10	31.5	30.40
15	26	25.92
20	22	21.96

Data for calculation: A= 5.8 x 10^{-7} m/s bar*; B=2.4 x 10^{-7} m/s; S=550 μm; π_d=44 bar; π_f=0.634 bar; C_d= 1M NaCl; C_f= 10 mM NaCl; k_d=$k_f \rightarrow \infty$;
*Remark: 1 m/(s bar)=3.6 x 10^6 L/(m^2 h bar)

5. Conclusions

By defining of the solute flux for every single mass transport layer makes possible to express the overall solute flux as well as the interface concentration of every single mass transport layer. This additional information enables the user to study more deeply and precisely the effect of the membrane characteristic parameters and operating conditions on the process performance. The change of the individual interface concentrations of the active membrane layer, which determines decisively the membrane performance, is significantly different as a function of the membrane parameters and operating conditions. The change of the feed side active layer's concentration is much more sensitive and varies in much wider range than that in the draw side membrane interface concentration as a function of the characteristic membrane properties. This can essentially ease to bring the membrane properties and operating conditions in harmony in interest of the process efficiency.

On the other hand, it was also shown that both the solute permeability and feed's solute concentration can strongly affect the membrane performance at even their very low values. It is also clearly illustrated that the knowledge of the single interface concentrations enables the user to predict the water flux more accurately.

Acknowledgement

The National Development Agency grant OTKA 116727 and GINOP-2.3.2-15-2016-00017 greatly acknowledged for the financial support.

Nomenclature

A	water permeability coefficient, m/(s atm), (m^3/m^{2}s atm)
B	salt permeability of the sponge layer, m/s
C	salt concentration, kg/m^3, g/L
D	fluid diffusion coefficient, m^2/s
J_s	solute transport rate, kg/m^{2}s
J_w	water flux, m^3/m^{2}s, m/s
k	diffusive mass transfer coefficient, m/s
$1/k_{ov}$	overall diffusive mass transport resistance, s/m
K	salt resistivity, s/m
R	rejection coefficient
R_g	gas constant, m^{3}atm/(K mol)
S	structural parameter, m
W	maximum energy density, W/m^2

Greek

β	transport coefficient, m/s
π	osmotic pressure, atm
δ	thickness of the fluid boundary layer, m
ε	porosity
τ	tortuosity
ΔP	hydraulic pressure difference, atm
ΔC_m	concentration difference of the selective layer, kg/m^3
$\Delta\pi_m$	osmotic pressure difference of the selective layer, atm

Subscript

d	bulk draw solution
f	bulk feed solution
m	draw side membrane layer
s	feed side active layer
sp	support layer

References

[1] B.C.Coday, N. Almaraz, T.Y. Cath, Forward osmosis desalination of oil and gas wastewater: impacts of membrane selection and operating conditions on process performance. J. Membr. Sci., 488 (2015) 40-55.

[2] D.L. Shaffer, N.Y. Yip, J. Gilron, M. Elimelech, Seawater desalination for agriculture by integrated forward and reverse osmosis: improved product water quality for potentially less energy, J. Membr. Sci., 415-416 (2012) 1-8.

[3] T.Y. Cath, M. Elimelech, J.R. McCutcheon, R.L. McGinnis, A. Achilli, A.R. Anastasio, A.E. Brady, I.V. Childress, N.T. Farr, J. Hancock, L.D. Lampi, M. Nghiem, M. Xie, N.Y. Yip. Standard methodology for evaluating membrane performance in osmotically driven membrane processes Desalination, 312 (2013) 31-38.

[4] A. Altaee, A. Sharif. Pressure retarded osmosis: advancement in the process application for power generation and desalination. Desalination, 356 (2015) 31-46.

[5] R.V. Linares, Z. Li, S. Sarp, Sz.C. Bucs, C, G. Amy, J.S. Vrouwenvelder, J.S. Forward osmosis niches in seawater desalination and wastewater reuse. Water Research, 66 (2014) 122-139.

[6] K. Lutchmiah, E.R. Cornelissen, D.J. Harmsen, J.W. Post, K.M. Lampi, M.H. Ramaekers, L.C. Rietveld, K.Roest,. Water recovery from sewage using forward osmosis. Water Sci. Technol., 64 (2011) 1443-1449.

[7] B. Jiao, A. Cassano, E. Drioli, Recent advances on membrane processes for the concentration of fruit juices: a review. J. Food Eng., 63 (2004) 303-324. [8] D.L. Shaffer, J.R. Werber, H. Jaramillo, S. Lin, M. Elimelech, Forward osmosis: where are we now?, Desalination, 356 (2015) 271-294.

[9] S. Zhao, L. Zou, C.Y. Tang, D. Mulcahy, Recent developments in forward osmosis: Opportunities and challenges, J. Membr. Sci. 396 (2012) 1-21.

[10] A.P. Straub, A. Deshmukh, M. Elimelech, Pressure-retarded osmosis for energy generation from salinity gradients: it is viable? Energy & Environ. Sci., 9 (2016) 31-48.

[11] G. O'Toole, L. Jones, C. Coutinho, C. Hayes, M. Napoles, A. Achilli, River-to-sea pressure retarded osmosis: Resource utilization in a full-scale facility, Desalination, 389 (2016) 39-51.

[12] C.F. Wan, T.S. Chung, Techno-economic evaluation of various RO-PRO and RO-FO integrated processes. Applied Energy. 212 (2018) 1038-1050.

[13] C. Klaysom, T.Y. Cath, T. Depuydt, I.F.J. Vankelecom, Forward and pressure retarded osmosis: potential solution for global challenges in energy and water supply. Chem. Soc. Rev. 42 (2013) 6959-6989.

[14] R.L. McGinnis, J.R. McCutheon, M. Elimelech, A novel ammonia-carbon dioxide osmotic heat engine for power generation. J. Membr. Sci., 305 (2007) 13-19.

[15] E., Nagy, J., Dudás, I., Hegedüs, Improvement of the energy generation by pressure retarded osmosis, Energy. 116 (2016) 1323-1333.

[16] J. Wang, D.S. Dlamini, A.K. Mishra, M.T. Pendergats, M.C.Y. Wong, B.B. Mamba, V. Freger, A.R.D. Verlifde, E. M.V. Hoek, A critical review of transport through osmotic membranes.J. Membr. Sci., 454 (2014) 516-537.

[17] K.L. Lee, R.W. Baker, H.K. Lonsdale, Membranes for power generation by pressure-retarded osmosis. J. Membr. Sci., 8 (1981) 141-147.

[18] N.N. Bui, J.T. Arena, J.R. McCutcheon, Proper accounting of mass transfer resistances in forward osmosis: Improving the accuracy of model predictions of structural parameters. J. Membr. Sci., 492 (2015) 289-302.

[19] E., Nagy, A general, resistance-in-series, salt- and water flux models for forward osmosis and pressure retarded osmosis for energy generation. J. Membr. Sci., 460 (2014) 71-81.

[20] S. Loeb, L. Titelman, E. Korngold, J. Freiman, Effect of porous support fabric on osmosis through a Loeb-Sourirajan type asymmetric membrane. J. Membr. Sci., 129 (1997) 243-249.

[21] A.L. Zydney, Stagnant film model for concentration polarization in membrane systems. J. Membr. Sci., 130 (1997) 275-281. [22] J.R. McCutcheon, M. Elimelech, Influence of concentrative and dilutive internal concentration polarization on flux behavior in forward osmosis. J. Membr. Sci., 284 (2006) 237-247.

[23] N.Y. Yip, A. Tiraferri, W.A. Phillip, J.D. Schiffman, L.A. Hoover, Y.C. Kim, M. Elimelech, Thin-film composite pressure retarded osmosis membranes for sustainable power generation from salinity gradients. Environ. Sci. Technol., 45 (2011) 4360-4369.

[24] A. Achilli, T.Y. Cath, E.A. Marchand, A.E. Childress, The forward osmosis membrane bioreactor: A low fouling alternative to MBR processes. Desalination 239 (2009) 10-21.

[25] M.J. Naguib, J. Maisonneuve, C.B. Laflamme, P. Pillay, Detailed membrane model for pressure-retarded osmotic power. Renew. Energy, 76 (2015) 619-627

[26] J. Maisonneuve, P. Pillay, C.B. Laflamme, Pressure-retarded osmotic power system model considering non-ideal effects. Renewable Energy 75 (2015) 416-424.

[27] C.F. Wan, T.-S. Chung, Osmotic power generation by pressure retarded osmosis using seawater brine as the draw solution and wastewater retentate as the feed. J. Membr. Sci. 479 (2015) 148-158.

[28] Z.L. Cheng, T.-S. Chung, Mass transport various membrane configuration in pressure retarded osmosis (PRO). J. Membr. Sci. 537 (2017) 160-176.

[29] A. Tiraferri, N.Y. Yip, W.A. Phillip, J.D. Schiffman, M. Elimelech, Relating performance of thin-film composite forward osmosis membranes to support layer formation and structure. J. Membr. Sci., 367 (2011) 340-352.

[30] R. Wang, L. Shi, C.Y. Tang, S. Chou. C. Qiu, A.G. Fane, Characterization of novel forward osmosis hollow fiber membranes. J. Membr. Sci., 355 (2010) 158-167.

[31] T.Y. Cath, A.E. Childress, M. Elimelech, Forward osmosis: principles applications and recent developments. J. Membr. Sci., 281 (2006) 70-87.

[32] T.-S. Chung, S. Zhang, K.Y. Wang, J. Su, M.M. Ling, Forward osmosis processes: Yesterday, today and tomorrow. Desalination, 287 (2012) 78-81.

[33] W.A. Phillip, J.S. Yong, M. Elimelech, Reverse draw solute permeation in forward osmosis: modeling and experiments. Environ. Sci. Technol. 44 (2010) 5170-5176.

[34] N.Y. Yip, M. Elimelech, Performance limiting effects in power generation from salinity gradients by pressure retarded osmosis. Environ. Sci. Technol., 45 (2011) 10273-10282.

[35] Y. Le, R. Wang, S. Qi, C. Tang, Structural stability and mass transfer properties of pressure retarded osmosis (PRO) membrane under high operating pressures. J. Membr. Sci., 488 (2015) 143-153.